Biochimica et Biophysica Acta 1808 (2011) 1129–1139

Contents lists available at ScienceDirect

Biochimica et Biophysica Acta

journal homepage: www.elsevier.com/locate/bbamem

# Acyl chain composition determines cardiolipin clustering induced by mitochondrial creatine kinase binding to monolayers

Ofelia Maniti [a], Mouhedine Cheniour [a], Marie-France Lecompte [b], Olivier Marcillat [a], René Buchet [a], Christian Vial [a], Thierry Granjon [a,*]

[a] Université de Lyon, Université Lyon 1, CNRS, UMR 5246, Institut de Chimie et Biochimie Moléculaires et Supramoléculaires, IMBL, F-69622 Villeurbanne, France
[b] INSERM U-563, Université Paul Sabatier, Faculté de Médecine de Rangueil, F-31062 Toulouse, France

ARTICLE INFO

*Article history:*
Received 11 August 2010
Received in revised form 21 December 2010
Accepted 10 January 2011
Available online 20 January 2011

*Keywords:*
Mitochondrial creatine kinase
Cardiolipin
Lipid domain
Acyl chain composition
Langmuir monolayer
Brewster angle microscopy

ABSTRACT

It has been recently shown that mitochondrial creatine kinase (mtCK) organizes mitochondrial model membrane by modulating the state and fluidity of lipids and by promoting the formation of protein–cardiolipin clusters. This report shows, using Brewster angle microscopy, that such clustering is largely dependent on the acyl chain composition of phospholipids. Indeed, mtCK-cardiolipin domains were observed not only with unsaturated cardiolipins, but also with the cardiolipin precursor phosphatidylglycerol. On the other hand, in the case of saturated dimyristoylphosphatidylglycerol and tetramyristoylcardiolipin, mtCK was homogeneously distributed underneath the monolayer. However, an overall decrease in membrane fluidity was indicated by infrared spectroscopy as well as by extrinsic fluorescence spectroscopy using Laurdan as a fluorescent probe, both for tetramyristoylcardiolipin and bovine heart cardiolipin containing liposomes. The binding mechanism implicated the insertion of protein segments into monolayers, as evidenced from alternative current polarography, regardless of the chain unsaturation for the phosphatidylglycerols and cardiolipins tested.



## 1. Introduction

Cardiolipin (CL, or diphosphatidyl glycerol), is a phospholipid present exclusively in membranes involved in energy production. Its acyl chain composition is specific to tissue and organism [1]. It has been shown to be an anchor and an essential platform for a number of proteins involved in fundamental processes such as energy production and apoptosis [2,3]. In muscle cells, CL contains mainly unsaturated lipids (up to 90% linoleoyl) with a symmetrical acyl chain distribution, namely tetralinoleoylcardiolipin, tetraoleoylcardiolipin and 1,3-dilinoleoyl-2,4-dioleoylcardiolipin [4,5].

Creatine kinase isoenzymes participate in energy transport between mitochondria and cytosol and ensure energy storage as phosphocreatine. The mitochondrial isoform (mtCK) can exist either as dimer or octamer, these two molecular species being interconvertible [6]. It is known to bind to the outer face of the inner mitochondrial membrane [7,8] only in its octameric state [6]. Membrane association is mainly due to electrostatic interactions between cardiolipin (CL) [9,10] and C-terminal positively charged residues ($Lys^{380}$, $Lys^{379}$ and $Lys^{369}$) exposed on top and bottom faces of the octameric cube [11]. Membrane binding is a two-step sequential process involving, in addition to electrostatic adsorption, a limited insertion of the protein between phospholipids [12]. Sarcomeric mitochondrial creatine kinase (mtCK) is very abundant in the intermembrane space. Based on specific activity measurements and immunologic titration it has been estimated that this enzyme represents about 1% of total mitochondrial proteins [13,14]. Thiol titration experiments suggest that mtCK and nucleotide translocator are in equimolar amounts [15], this last protein accounting for 5% of total mitochondrial proteins [16]. mtCK is exclusively restricted to the mitochondrial intermembrane space, this submitochondrial compartment representing less than 5% of mitochondrial proteins [17]. mtCK plays a role in the formation and stabilization of contact sites between outer and inner mitochondrial membranes [18,19], in regulating the mitochondrial permeability transition pore [20–23]. Moreover, mitochondria from transgenic mice expressing mtCK in liver cells, which are normally devoid of this enzyme, show an increased number of contact points [24]. Silencing mtCK RNA results in severe alterations of mitochondrial morphology [25], pointing to a structural role of this enzyme in mitochondria.

mtCK binding to bovine heart CL-containing liposomes decreases the fluidity of the membrane and induces small structural changes in the protein [26]; it also provokes specific CL phase separation in phosphatidylethanolamines (PE)–CL mixtures [27]. We have previously shown that mtCK interaction with phospholipid monolayers mimicking the inner mitochondrial membrane conditions induces formation of organized CL-rich complexes [28]. Since the level of

* Corresponding author at: ICBMS/UMR-CNRS 5246, Bât. Raulin, Université Claude Bernard Lyon 1; 43, bd. du 11 Novembre 1918, F-69622 Villeurbanne, France. Tel.: +33 472431503; fax: +33 472431557.
*E-mail address:* thierry.granjon@univ-lyon1.fr (T. Granjon).

0005-2736/$ – see front matter © 2011 Elsevier B.V. All rights reserved.
doi:10.1016/j.bbamem.2011.01.005

unsaturated fatty acids in CL and in its precursor phosphatidylglycerol (PG) plays an important role in mitochondrial physiology [29,30], we investigated mtCK interaction with model membranes containing CL with different acyl chain composition. Our findings indicate that mtCK binding to both unsaturated bovine heart CL and saturated tetramyristoylcardiolipin (TMCL) induces an overall fluidity decrease in CL or TMCL-containing liposomes and involves protein insertion between lipids. Highly organized lipid–protein clusters are, however, only observed with unsaturated cardiolipin, or with unsaturated phosphatidylglycerol. The formation of CL-enriched clusters seems thus to be dependent on lipid chain properties.

## 2. Experimental procedures

### 2.1. Protein expression and purification

Recombinant octameric rabbit heart mtCK (340 kDa) was purified as described elsewhere [31]. The purified enzyme was stored in 20 mM Tris–HCl, 0.1 mM EDTA, and 0.2 mM DTT pH 7.4 buffer, at a protein concentration of 0.2 g/L, as determined by the Lowry method using bovine serum albumin as the standard.

Protein activity was checked using pH-stat technique [32] and was found to be independent of the presence of liposomes, whatever their composition in phospholipids.

### 2.2. Film formation and surface pressure measurements for Brewster angle microscopy (BAM) and polarization modulation infrared reflexion spectroscopy (PM-IRRAS)

A circular Teflon trough (Riegler & Kirstein, Potsdam, Germany) with a volume of 30 mL and a surface of 27 $cm^2$ was used. The trough was filled with 20 mM Tris–HCl pH 7.4 buffer. Phospholipid monolayers were formed on a clean air–buffer interface by spreading the phospholipids dissolved in chloroform to reach lateral surface pressures between 30 and 35 mN/m. After pressure stabilization, mtCK was injected in the subphase, using a Hamilton syringe, at a final concentration of 4 nM. Measurements were taken at 21 °C.

### 2.3. BAM measurements

A commercial Brewster angle microscope manufactured by Nanofilm Technology (Göttingen, Germany) was used to determine the morphology of phospholipid films [33,34] in the absence or presence of protein. Images size was 430 × 540 μm with 2-μm spatial resolution. The measurements were performed at different shutter speeds ranging from 1:50 to 1:2000 s to adapt to different illumination levels. After camera calibration, the reflectance ($I$) was determined from the measured intensity parameter for different shutter speeds, the gray level (GL) [35,36]. For ultra thin films, the reflectance depends on both the thickness and refractive index of the monolayer:

$$I \propto \lambda d^2 n^2$$

where λ is the laser wavelength, $d$ is the film thickness and $n$ is the refractive index of the interfacial film. For a measured reflectance and at a given refractive index the BAM software allowed us to determine the average or local thickness of the film, as previously described [28].

### 2.4. Fluorescence spectroscopy measurements

Aliquots of TMCL and CL in chloroform solution were combined in 3:1 molar ratio with egg yolk PC and in a 200:1 molar ratio with Laurdan. Large unilamellar vesicles were prepared by hydration and extrusion as previously described [26].

Fluorescence measurements were performed with a Hitachi F4500 fluorometer (150-WXe). The excitation and emission band-pass values were 5 nm. Spectra were recorded 20 min after addition of mtCK (2 μg) to the liposomes (5 μg of phospholipids), using a 1-cm path length quartz cuvette, thermostated at 37 °C. All fluorescence spectra were corrected for the baseline spectra of the buffer solution to remove the contribution of the Raman band. Laurdan emission spectra were recorded between 400 and 600 nm using a 350-nm excitation wavelength in the absence or presence of 2 μg mtCK in 20 mM Tris–HCl buffer (pH 7.4). The excitation generalized polarization ($GP_{ex}$) was calculated as

$$GP_{ex} = (I_{440} - I_{490}) / (I_{440} + I_{490})$$

where $I_{440}$ and $I_{490}$ are the fluorescence intensities at the maximum emission wavelength in the ordered (440 nm) and in disordered (490 nm) phase at a 350-nm excitation wavelength.

### 2.5. Fourier transformed infrared measurements

Liposomes were prepared as previously described [26]. For assay with protein, the liposome suspension (160 μg of phospholipids) was mixed with 200 μg of lyophilized enzyme in 20 mM Tris–HCl–$^2H_2O$ ($p^2H$ 7.4), and then incubated at 21 °C for 20 min. The removal of unadsorbed protein was performed by centrifugation at 160,000 × $g$ for 60 min (Beckman Airfuge). The pellet was resuspended in 24 μL of Tris–$^2H_2O$ buffer.

The $p^2H$ was measured with a glass electrode and was corrected by a value of 0.4 according to Glasoe and Long [37]. Samples were loaded between two $CaF_2$ circular cells, with a 50-μm Teflon spacer. FTIR spectra were recorded with a Nicolet 510 M FTIR spectrometer which was continuously purged with dry air. The infrared cell was thermostated with a water circulation bath. The nominal spectral resolution was 4 $cm^{-1}$; 256 scans were collected and co-added per sample spectrum, and Fourier-transformed for each sample. Every infrared spectrum was representative of at least three independent measurements. The infrared spectra of the corresponding buffer and residual water vapor were subtracted from the infrared spectrum of the sample.

### 2.6. Alternative current polarographic measurements

Admittance measurements, as a special use of alternative current polarography at low frequency, allow measurements of the differential capacity ($C$) of a mercury electrode in contact with a lipid monolayer. Defined as the second derivative of the surface tension with respect to the potential [38], the differential capacity is highly sensitive to minute variations of the surface pressure. This has made the method valuable for monitoring the interaction of hydrosoluble molecules with condensed phospholipid monolayers [12,39–42]. Electrochemical measurements were carried out as described elsewhere [12,39] in a Metrohm polarographic cell. Oxygen was displaced from the solution by argon. The working electrode was a hanging mercury drop that was formed at the extremity of a thin capillary tip of the Metrohm electrode device and positioned in contact with the phospholipid monolayer. An Ag/AgCl saturated KCl electrode and a platinum gauge were respectively the reference and the counter-electrode. Potentials are reported versus the Ag/AgCl, sat. KCl reference electrode. The starting potential was chosen in the stable region of the monolayer, i.e., at −0.2 V. Dried phospholipid samples were dissolved in hexane and spread at the surface of the electrolyte (0.05 M NaCl, 20 mM Tris–HCl, pH 7.4), until the differential capacity becomes stable and constant over a large potential range around the potential of zero charge of the electrode (pzc, −0.45 V) as described previously [41]. In our experiments, 0.2 μg/$cm^2$ CL and TMCL were required to ensure that buffer surface was fully covered by the lipid

monolayer [12]. mtCK was injected beneath the monolayer at 4 nM final concentration. The *C* versus *E* curve in the presence of protein was recorded 1 h after protein injection.

### 2.7. PM-IRRAS measurements

Interface studies of mtCK in the absence or presence of lipid monolayers at 30–35 mN/m lateral surface pressure were performed at 21 °C by PM-IRRAS measurements as elsewhere described [43–46]. The spectra were recorded on a Nicolet Nexus 870 Fourier transform infrared spectrometer (Thermo Scientific, Madison, WI). The light beam was reflected towards the optical bench by a mobile mirror. It was then polarized by a ZnSe polarizer and directed towards a photoelastic modulator that modulated the beam between a parallel (p) and a perpendicular (s) polarization. The light beam was directed towards the monolayer at an angle of 75° and reflected on a photovoltaic MCT-A detector cooled at 77 K. The detected signal was then processed to obtain the differential reflectivity spectrum:

$$\Delta R/R = J_2 \times \left(R_p - R_s\right) / \left(R_p + R_s\right)$$

where $J_2$ is the Bessel function depending only on the photoelastic modulator, while $R_s$ and $R_p$ are the parallel and perpendicular reflectivities, respectively. To remove the Bessel function contribution as well as that of the water absorption, the monolayer spectrum was divided by that of the pure subphase. Then 1024 scans were summed at a resolution of 8 $cm^{-1}$ for pure mtCK, pure lipid monolayers or lipid monolayers in the presence of mtCK. To obtain the spectra of lipid bound mtCK, the spectra of the pure lipids were subtracted from those of the mixed monolayers. Each spectrum is the average of at least three independent experiments. Each experiment consisted of three series of scans.

## 3. Results

### 3.1. mtCK interaction with unsaturated or saturated acyl chain cardiolipins visualized by Brewster angle microscopy

#### 3.1.1. mtCK interaction with bovine heart unsaturated cardiolipin

A lateral surface pressure between 30 and 35 mN/m was obtained by spreading specific phospholipids at the air buffer interface, as stated in the Experimental procedures section. When injected beneath a monolayer composed of CL extracted from bovine heart, characterized by a high percentage of unsaturated species (over 80%, mainly linoleyl (C18:2)), mtCK induced formation of bright domains (Fig. 1) with increased thickness or/and refractive index. The bright regions progressively increased in number and in size (Fig. 1b–f) to finally adopt specific arborescent shapes. Using a refractive index of 1.46, which is characteristic of a fluid phospholipid film, we estimated an average film apparent thickness increase from 1.8 nm in the absence of protein to 2.5 nm three and a half hours after protein injection (Fig. 1f) because of the interaction between mtCK molecules and the negatively charged lipid head groups on the lower face of the monolayer. The gray level measured locally on the bright areas of the image allowed us to estimate a local thickness of the clusters attaining 12 nm.

#### 3.1.2. Comparison of mtCK interaction with unsaturated tetraoleoylcardiolipin (TOCL)

At BAM lateral resolution (μm), the TOCL monolayer (unsaturated chains of 18 carbons) had a rather homogeneous aspect and was highly fluid (Fig. 2a). The average monolayer thickness was estimated at 2 nm. When mtCK was injected beneath the monolayer, an increase in the image gray level together with formation of bright spots was recorded. The increase in the gray level corresponded to a monolayer thickness variation from 2 nm in the absence of protein to 3 nm measured 3h30 after mtCK injection. Locally, these bright clusters attained more important thickness, with values comparable to those

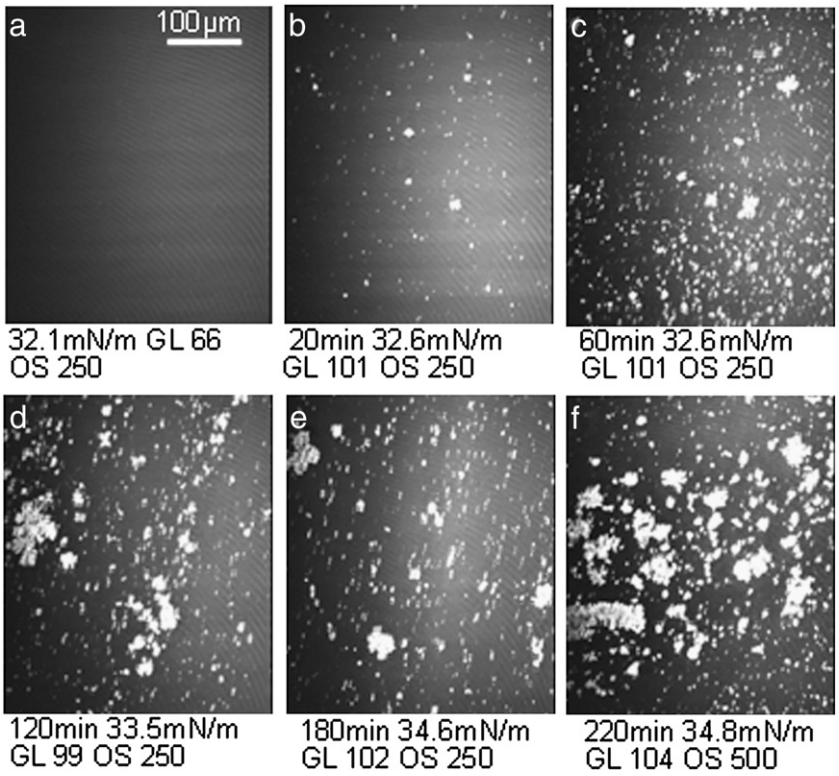


**Fig. 1.** BAM images of a bovine heart CL monolayer spread at 32 mN/m before (a) and after mtCK injection (b–f). Incubation time after mtCK injection, lateral surface pressure in mN/m, gray level (GL) and obturation speed (OS) are indicated below each image.

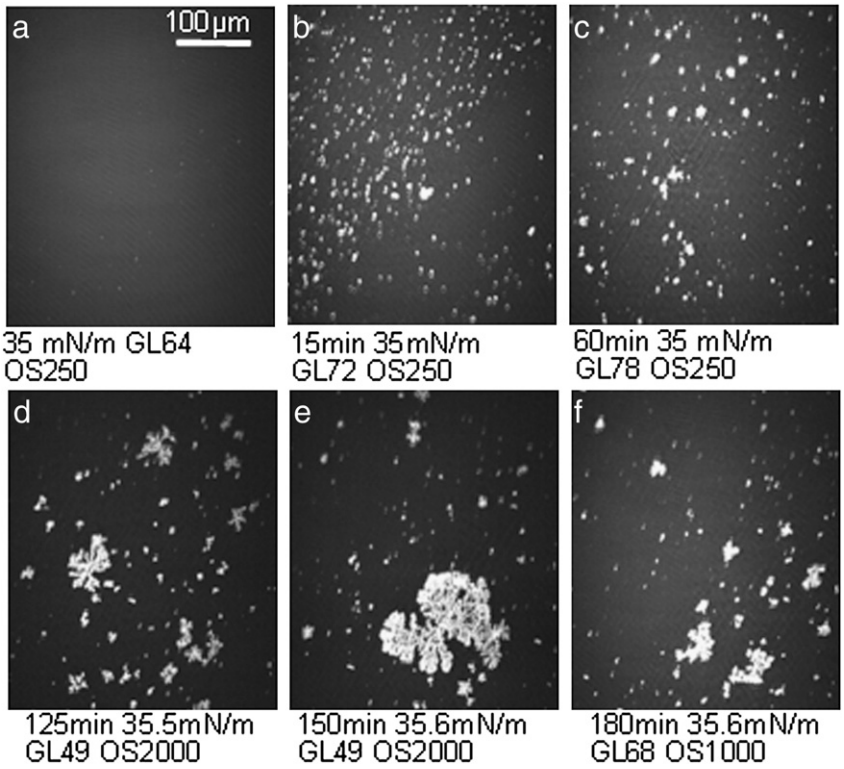


**Fig. 2.** BAM images of a TOCL monolayer spread at 35 mN/m before (a) and after mtCK injection (b–f). Incubation time after mtCK injection, lateral surface pressure in mN/m, gray level (GL) and obturation speed (OS) are indicated below each image.

recorded for the bovine heart CL (10 to 12 nm). They progressively grew in size and also adopted arborescent fractal shapes (Fig. 2e, f).

### *3.2. mtCK interaction with a liquid condensed saturated tetramyristoylcardiolipid (TMCL) monolayer*

Under the buffer conditions (Tris–HCl 20 mM, pH 7.4, 21 °C), TMCL (saturated chains of 14 carbons) isotherm presents a liquid expanded–liquid condensed (LE–LC) phase transition around 15 mN/m (not shown). TMCL was spread at the air–buffer interface at a surface pressure of 32 mN/m, which is above the LE–LC phase transition. This monolayer, corresponding to a liquid condensed state, also had a homogeneous aspect (Fig. 3a), but was brighter and more rigid than the CL or TOCL monolayers described above. An average thickness of 2.5 nm was estimated using a refractive index of 1.5, more adapted to a monolayer in a liquid condensed phase [47]. The addition of mtCK beneath the TMCL monolayer induced a regular and strong increase in the gray level of the images, thus indicating an increase in monolayer thickness, which attained 5.6 nm when measured 3h30 after protein injection. In contrast to the observations made with CL and TOCL, the aspect of the TMCL monolayer was homogeneous without distinct bright spots (Fig. 3b–f), at least at Brewster angle resolution (µm).

### *3.3. mtCK interaction with a liquid expanded saturated tetramyristoylcardiolipid monolayer*

We analyzed the interaction of mtCK at 10 mN/m surface pressure which corresponds to a liquid expanded (LE) phase. As shown in Fig. 4, before mtCK injection TMCL monolayer was homogeneous (Fig. 4a). Liquid condensed domains begin to form 90 min after protein addition (Fig. 4b) and progressively grew in size for 150 min after injection (Fig. 4c). During this time lapse the average thickness of the monolayer increased from 1.1 to 1.9 nm. The estimated thickness of the liquid condensed domain was of 2.2 nm, while the thickness of the liquid expanded regions was estimated at 1.5 nm.

For longer incubation, the size of the domains did not evolve, but a drastic increase in the average thickness of the monolayer up to 4.3 nm was recorded (Fig. 4d to f).

### *3.4. mtCK interaction with phosphatidylglycerols*

The influence of the polar head group on the interaction between mtCK and negatively charged phospholipids was checked with saturated synthetic dimyristoylphosphatidylglycerol (DMPG) and egg yolk PG. The DMPG monolayer, which in our conditions is in a liquid expanded (LE) state, showed a homogenous aspect (Fig. 5, top panels, a). Three hours after protein injection, although well differentiated domains did not appear (Fig. 5, top panels, b, c), the global brightness of the film increased, which indicates a variation of the average thickness from 1.5 to 3.2 nm. Egg yolk PG monolayer was homogeneous with an estimated thickness of 2 nm (Fig. 5, bottom panels, a). In the hours following mtCK injection, bright irregular domains formed and their size and number increased with time (Fig. 5, bottom panels, b, c). However, these domains were smaller than those observed with CL monolayers. The average thickness of the monolayer increased from 2 to 3.2 nm.

### *3.5. mtCK induced modifications in membrane fluidity*

To evidence possible modifications in membrane structure/organization/fluidity induced by mtCK interaction with unsaturated (bovine heart CL) or saturated cardiolipins (TMCL), we used a fluorescent probe, Laurdan. When inserted in lipid membranes, Laurdan distributes equally between lipid phases and displays a phase-dependent emission spectral shift, from 440 nm in the ordered lipid phase to 490 nm in the disordered lipid phase [48–50]. This effect is attributed to the reorientation of water molecules present at the lipid interface near Laurdan's fluorescent moiety, i.e., water dipolar relaxation process [51].

Laurdan emission spectra in PC/CL (3:1) or PC/TMCL (3:1) vesicles were recorded with an excitation wavelength of 350 nm and in the

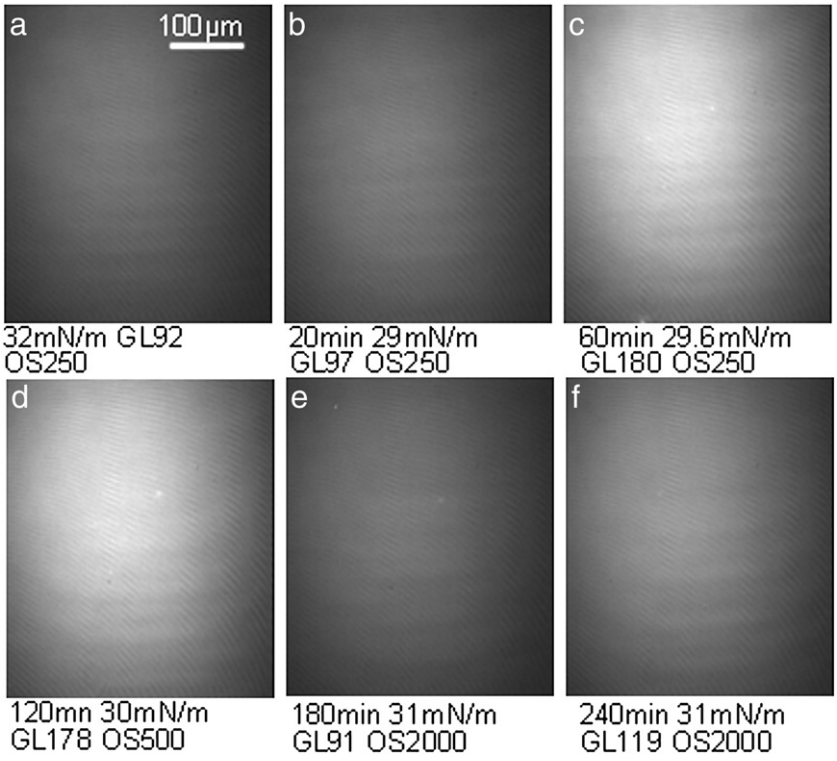


**Fig. 3.** BAM images of a TMCL monolayer spread at 32 mN/m before (a) and after mtCK injection (b–f). Incubation time after mtCK injection, lateral surface pressure in mN/m, gray level (GL) and obturation speed (OS) are indicated below each image.

presence or absence of mtCK. Emission spectra of the PC/CL (3:1) lipid mixture in the absence of protein were dominated by the emission of Laurdan molecules in the fluid phase (not shown). The presence of mtCK induced an increase in the fluorescence emission intensity at 440 nm, which indicated that membrane became more ordered.

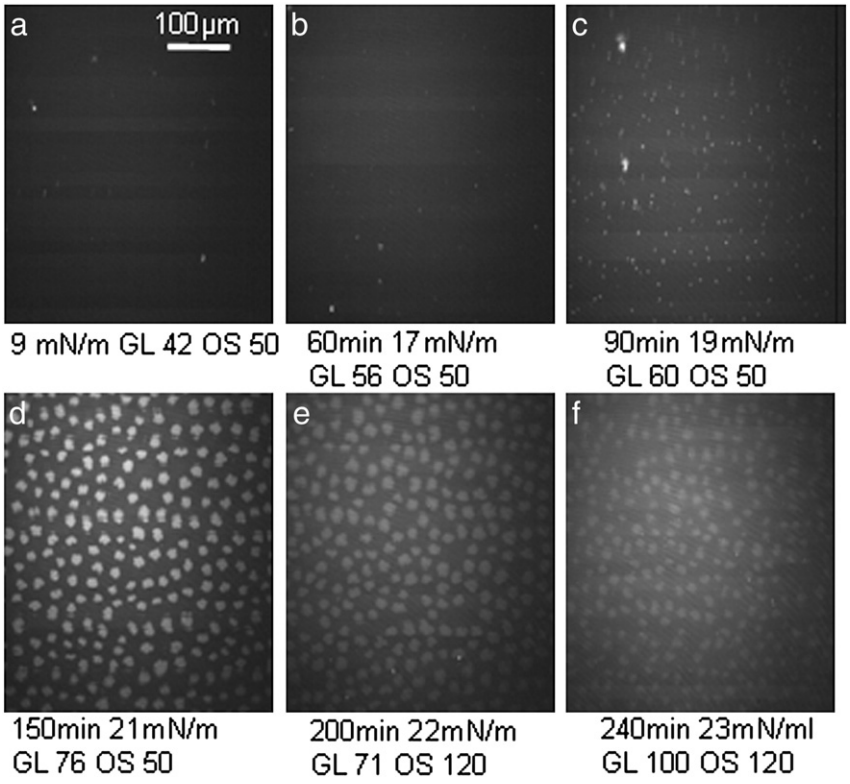


**Fig. 4.** BAM images of a TMCL monolayer spread at 10 mN/m before (a) and after mtCK injection (b–f). Incubation time after mtCK injection, lateral surface pressure in mN/m, gray level (GL) and obturation speed (OS) are indicated below each image.

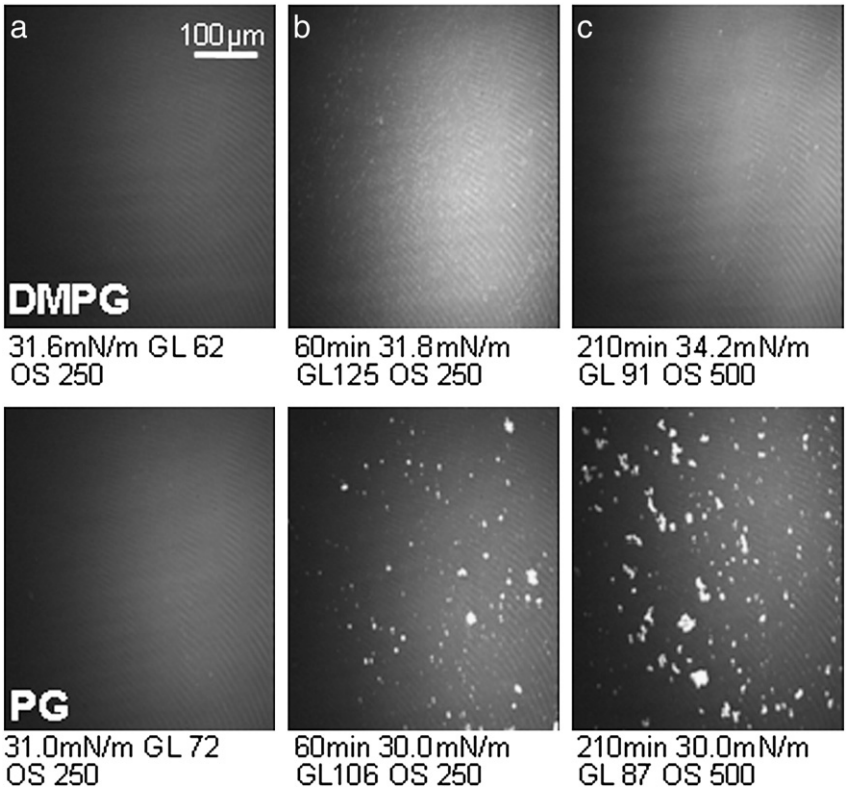


**Fig. 5.** BAM images of DMPG (top) or egg yolk PG monolayers (bottom) spread at 31 mN/m before (column a) and after mtCK injection (columns b and c). Incubation time after mtCK injection, lateral surface pressure in mN/m, gray level (GL) and obturation speed (OS) are indicated below each image.

This was confirmed by the increase in $GP_{ex}$ from $-0.294 \pm 0.004$ in the absence of protein to $-0.257 \pm 0.01$ in its presence (Fig. 6a), corresponding to a $-0.037 \pm 0.005$ delta $GP_{ex}$ (Fig. 6b, white rectangle). For the PC/TMCL (3:1) mixture, Laurdan fluorescence spectrum was also dominated by the emission of the fluid phase at 490 nm with a $GP_{ex}$ of $-0.241 \pm 0.005$. mtCK induced a distinct increase in the $GP_{ex}$ value of PC/TMCL (3:1) liposomes, from $-0.241 \pm 0.005$ to $-0.201 \pm 0.004$ (Fig. 6a), leading to a delta $GP_{ex}$ of $-0.040 \pm 0.005$ (Fig. 6b, black rectangle). Thus, mtCK had an ordering effect both on CL and TMCL, at a similar extent.

This ordering effect was confirmed by infrared measurements. C—H stretching wavenumbers of the lipid hydrocarbon chains can be used as a measure of chain order. mtCK binding to PC/TMCL 3:1 liposomes induced a shift of symmetrical and asymmetrical $CH_2$ bands from 2852 to 2850 $cm^{-1}$ (not shown) and from 2922 to 2919 $cm^{-1}$, respectively (Fig. 7). A similar spectral shift was reported for mtCK binding to CL-containing liposomes [26] and reflects a higher degree of ordering of hydrocarbon chains of both TMCL and CL in the presence of mtCK.

### 3.6. Effect of mtCK on the differential capacity of phospholipid monolayers

Differential capacity ($C$) of the hanging mercury drop electrode in contact with different negatively charged phospholipids was recorded as function of electric potential ($E$) applied between the working and the reference electrode (Fig. 8). This allowed us to follow perturbations in lipid monolayer organization in response to the applied electric potential and assess protein-induced modifications. Two regions of interest were analyzed. The first one, between −0.2 and

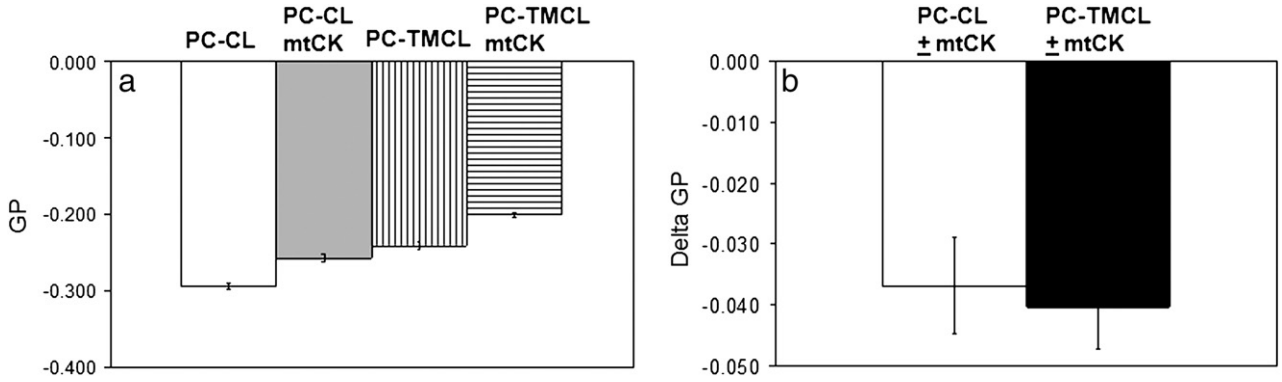


**Fig. 6.** Modifications in liposome-Laurdan generalized polarization values induced by mtCK binding: a. Calculated $GP_{ex}$ values for PC/CL (3:1) liposomes in the absence (white rectangle) or presence of mtCK (gray rectangle) and for PC/TMCL (3:1) liposomes in the absence (rectangle with vertical lines) or presence of mtCK (rectangle with horizontal lines). b. Variation of excitation GP for PC/CL (3:1) liposomes (white rectangle) or PC/TMCL (3:1) (black rectangle) liposomes in presence of mtCK. $\Delta GP_{ex}$ = excitation GP in the presence of mtCK minus excitation GP in the absence of mtCK.

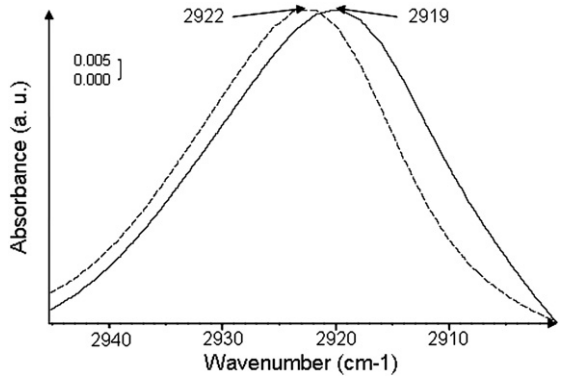


**Fig. 7.** Infrared spectra in the region of the asymmetric $CH_2$ stretching vibration of PC/TMCL (3:1) liposomes in the absence (dotted line) or presence of mtCK (solid line).

−0.7 V includes the potential of zero charge of the electrode (pzc) (−0.45 V). In our conditions, as previously described [12,28], in the absence of mtCK, the value of *C* for the lipid monolayer was stable at its lowest value (1.6 μF/cm$^2$), indicating that the entire available surface was covered with lipids. Upon protein addition, an increase in *C* at pzc, from 1.6 to 3.2 μF/cm$^2$, indicated protein insertion between lipids [39].

The second region of interest on the *C* vs. *E* curve corresponds to more negative potentials (−0.9 to −1.4 V) for which the *C* vs. *E* curve showed two main lipid specific peaks of very fine shape at −1 and −1.2 V (Fig. 8a, solid line). Addition of mtCK induced drastic modification on the *C* vs. *E* curve of the CL monolayer (Fig. 8a, dotted line), indicating that lipid behavior was severely altered by the protein.

For a TMCL monolayer in the absence of protein, at the pzc, a stable value of 2.2 μF/cm$^2$ was obtained for *C*. The profile of the *C* vs. *E* curve for a TMCL monolayer presented striking differences compared to that of the CL (Fig. 8b, solid line). This was expected since lipid behavior in response to potential variation is highly dependent on acyl chain composition [52]. Namely, TMCL monolayer rearrangements at the electrode occurred at less negative potentials, marked by the presence of a double peak at −0.85 V for TMCL instead of the single peak at −1 V for bovine heart CL. Further variation of the potential to more negative values induced other rearrangements, as indicated by the

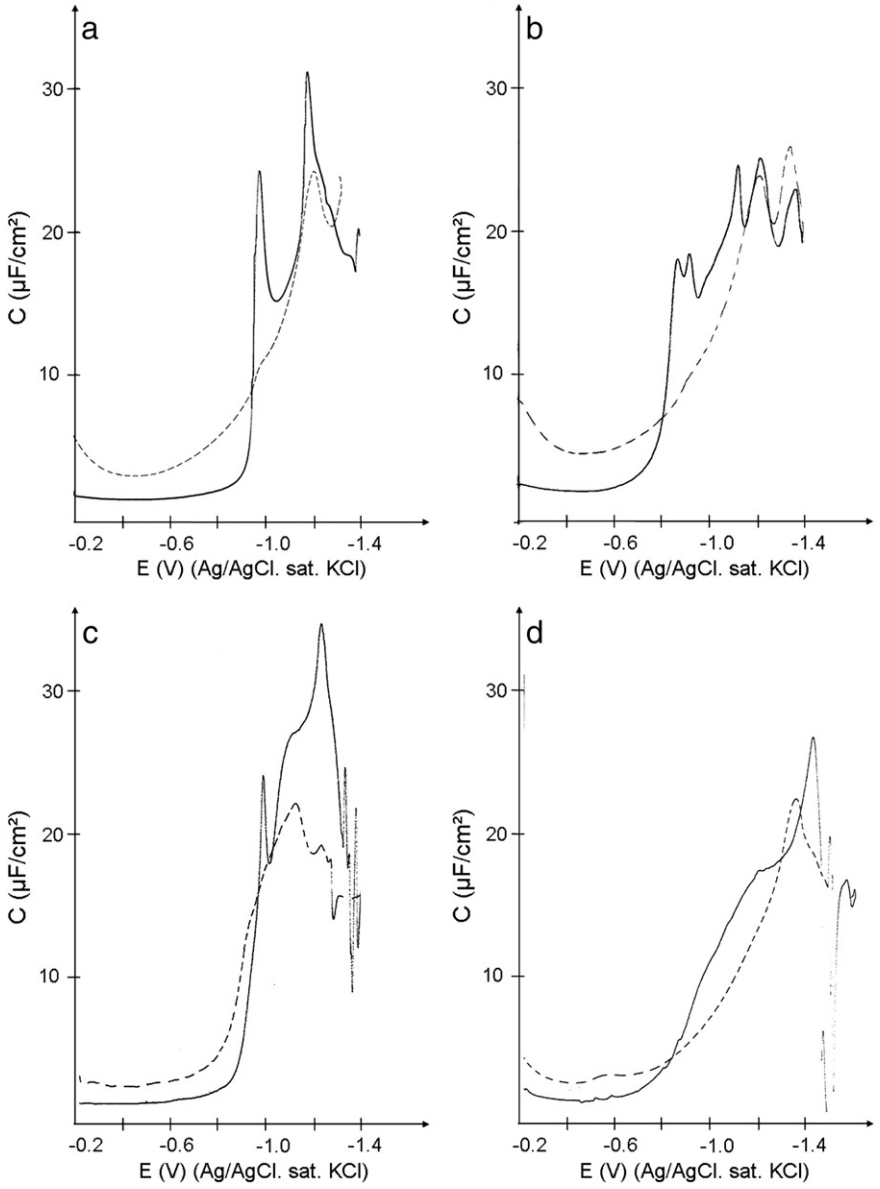


**Fig. 8.** Differential capacity versus electrical potential curves obtained with a hanging mercury drop electrode in contact with the monolayer before (solid line) or after mtCK injection (dotted line): a. bovine heart CL; b. TMCL; c. egg yolk PG; d. DMPG monolayers.

multiple peaks present on the *C* vs. *E* curve. The presence of mtCK induced a strong increase in *C* at the pzc from 2.2 to 4.5 μF/cm$^2$, in the same proportion than with CL (Fig. 8b, dotted line), indicating that protein segments inserted between lipids. A drastic modification of the peaks was also recorded. In particular, the double peak around −0.85 V disappeared.

We also tested whether the capability of mtCK to insert into monolayers is specific to cardiolipin or is also observed for monolayers constituted of phosphatidylglycerol.

In the absence of protein, the differential capacity of a monolayer constituted of unsaturated egg yolk PG was low and constant (1.4 μF/cm$^2$) over the −0.2 to −0.7 V potential range. Peaks appeared around −0.9 and −1.2 V with a shoulder at −1.1 V.

mtCK interaction with this monolayer induced an increase in the value of *C* at pzc from 1.4 to 2.7 μF/cm$^2$. This attested that mtCK was also able to insert between PG molecules. Meanwhile, the peaks at −0.9 and −1.2 V strongly diminished.

The differential capacity of a pure DMPG monolayer at pzc attained a value of 1.6 μF/cm$^2$. At further potential variation a large shoulder was observed in the −0.8 to −1.2 V range, whereas a sharp peak was present at −1.4 V. In the presence of mtCK, the value of the differential capacity at pzc increased from 1.6 to 2.9 μF/cm$^2$, while it decreased in the region of the shoulder. A peak was present on the *C* vs. *E* curve at −1.3 V. Those results also point to an insertion of mtCK between DMPG molecules.

### 3.7. Protein orientation in the presence of saturated and unsaturated lipids

PM-IRRAS spectrum of mtCK in interaction with a TMCL monolayer at a lateral surface pressure between 30 and 35 mN/m was compared with that of mtCK in the presence of a bovine heart CL monolayer (Fig. 9). The amide-I/amide-II ratio measured on the PM-IRRAS spectrum was taken as an approximate measure of the relative orientation of the average carbonyl peptide backbone with respect to the interface plane [43,46]. An average of nine experimental data allowed us to calculate an amide-I/amide-II ratio of $2 \pm 0.03$ for the protein in the presence of the TMCL monolayer (Fig. 9, black, solid line) instead of $1.6 \pm 0.05$ in the presence of a bovine heart CL monolayer (Fig. 9, dotted line) [28]. According to simulation models [46], and assuming that the intensity of the amide-I band centered around 1650–1660 cm$^{-1}$ reflected mostly the carbonyl peptide backbone of α-helices and neglecting the contribution of other secondary structures [28], these values can be modeled [46] to an overall orientation of the α-helices tilted from the interface plane by 40° in the presence of a TMCL monolayer, instead of 45° in the presence of a bovine heart CL monolayer. We also compared the PM-IRRAS spectra of mtCK in interaction with egg yolk PG and DMPG monolayers at the same lateral surface pressure. For both lipids, an amide-I/amide-II ratio of $2 \pm 0.06$ was determined, which again corresponded to an average tilt of α-helices from 30° to 40° from the interface plane.

## 4. Discussion

### 4.1. Changes of morphology and apparent thickness of cardiolipin or phosphatidylglycerol monolayers after mtCK binding

Mitochondrial inner membrane cardiolipin is characterized by a high percentage of unsaturated fatty acids. In muscle cells, linoleyl chains attain extremely high percentages, up to 90% [4,5]. Although the role of this particular composition is not well established, it has been related to CL capability to interact with transmembrane proteins. In this report, we analyzed the interaction between different types of cardiolipin and a peripheral protein known to bind to the outer face of the inner mitochondrial membrane, mtCK. We have previously shown that mtCK is able to organize CL molecules, inducing a time-dependent phospholipid clustering on monolayers containing either 100% bovine heart CL or mixture of phospholipids mimicking the composition of the inner mitochondrial membrane [28]. In view of the amount of mtCK in the intermembrane space, its interaction with the membrane is likely to affect CL distribution and thus, membrane organization. Moreover, mtCK is able to modify lipid phase transitions and the morphology of liquid condensed domains in monolayers, favoring and stabilizing the condensed phase [53,54].

In the absence of protein, all the lipid monolayers observed by BAM indicated a rather homogenous surface at the instrument lateral resolution (about 2 μm). The injection of mtCK beneath bovine heart CL (Fig. 1) or TOCL (Fig. 2) monolayers induced formation of bright irregularly shaped domains with important local thickness (10–12 nm), 5 to 6 times higher than that of the pure monolayer (1.8–2 nm). Since mtCK is a cubic protein of $93 \times 93 \times 86$ Å [55], this indicates the formation of lipid–protein complexes, where mtCK binds to cardiolipin's charged head group beneath the lipid layer. The intensity of the clustering effect is higher with the bovine heart CL monolayer (mainly constituted of C18:2 chains) than with the TOCL monolayer (constituted of C18:1 chains). The shape of the domains evidences a high line tension between rigid, organized lipid–protein complexes and a rather fluid environment [51]. A compact organization of the bright clusters is also indicated by thickness estimation in ranges consistent with the height of a CL–mtCK complex.

### 4.2. Distinct effects of mtCK binding at liquid condensed and liquid expended states of TMCL monolayers

Concerning the TMCL monolayer in a liquid condensed (LC) state, addition of mtCK induced a strong but homogeneous increase in the average thickness, from 2.6 to 5.6 nm (Fig. 3). When injected beneath

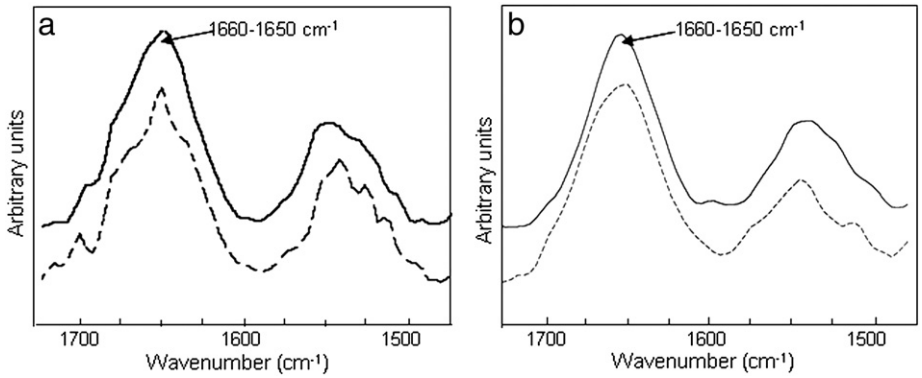


**Fig. 9.** PM-IRRAS spectra of mtCK in the presence of phospholipid monolayers: (a) TMCL monolayer (black, solid line) or bovine heart CL monolayer (dotted line); (b) DMPG monolayer (black, solid line) or egg yolk PG monolayer (dotted line).

a TMCL monolayer in a liquid expanded state, mtCK induced lipid phase transition with the formation of liquid condensed domains (Fig. 4). This phenomenon can be related to mtCK ability to shift the lipid LE–LC phase transition towards lower surface pressure, as previously described [53,54]. This is confirmed by fluorescence (Fig. 6), as well as infrared spectroscopy findings (Fig. 7) which indicated that mtCK binding decreased membrane fluidity of both TMCL and bovine heart CL-containing liposomes. The thickness of the LC domains attained 2.2 nm, much lower than the thickness measured for bovine heart CL monolayers after mtCK addition (12 nm).

For longer incubation period, a second phenomenon occurred, i.e. an overall thickness increase from 1.9 to 4.3 nm. During this period the liquid condensed domains underwent little change. This was reminiscent of the overall thickness increase observed with liquid condensed TMCL monolayer. No compact mtCK–cardiolipin clusters were observed.

The clustering of CL–mtCK complexes is therefore dependent on the composition of the acyl chains and on the fluidity of the monolayer: very intense with linoleoyl species, less intense, but nevertheless important, with oleoyl species and absent, at least at BAM instrument resolution, with myristoyl species. These observations indicate that the types of CL present in healthy muscle cells, characterized by long and unsaturated acyl chains, are more prone to cluster upon binding with mtCK than modified cardiolipins present in some pathological tissues.

### 4.3. Changes of morphology and apparent thickness of phosphatidylglycerol monolayers after mtCK binding

Although CL is the binding partner of mtCK in the inner mitochondrial membrane, mtCK is also able to interact with liposomes and monolayers containing CL precursor, phosphatidylglycerol. The morphology of phosphatidylglycerol monolayers upon mtCK binding is also dependent on acyl chain composition. When the monolayer was constituted of DMPG (single anionic head group and 14 carbon-long saturated chains) a global increase in the average thickness of the surface layer from 1.5 to 2.4 nm was observed but without discrete domains (Fig. 5, top). On the contrary, after mtCK injection beneath a monolayer constituted of natural, unsaturated PG, discrete bright domains were formed (Fig. 5, bottom), with similar shapes and thickness to those observed with bovine heart CL. As both phospholipids, PG and DMPG, have the same polar head, the differences observed in these experiments were attributed to differences in monolayer fluidity due to their difference in length and in the unsaturation degree of their acyl chains. It is worth noticing that defects in CL-synthase do not induce gross mitochondrial morphological alterations, suggesting that PG can partially take over the role of CL in mitochondrial morphology [56]. Those results are in line with our observation regarding PG ability to form proteo-lipid complexes. However, mtCK-PG complexes were smaller than those observed with unsaturated cardiolipins. This finding can be attributed either to differences in the structure of the polar head or to the lower unsaturation of egg yolk PG (33% C18:1, 14% C18:2, 36% C16:0, 10% C18:0) as compared to that of the bovine heart CL or TOCL.

### 4.4. Protein insertion into monolayers—Differential capacity measurements

We tested mtCK ability to insert into monolayers by measuring the differential capacity of a hanging mercury drop electrode in direct contact with a lipid monolayer at high lateral pressure upon protein interaction [39]. This method can be used to assess whether a molecule injected in the subphase adsorbs at the charged lipid head group or inserts into the lipid monolayer [12]. Measurements were performed on bovine heart CL and TMCL around the pzc, where there is no or negligible superimposed electric field which could affect the interaction. The addition of mtCK beneath bovine heart CL or TMCL monolayers induced a significant increase in $C$ around the pzc (Fig. 8). This increase is characteristic of a perturbation of the continuity of the dense phospholipid layer and, consequently, corresponds to a certain degree of protein insertion into the monolayer [12,39,40]. Of interest, the insertion of mtCK into the monolayer is observed for both bovine heart CL and TMCL, indicating that the insertion is independent on acyl chain composition.

Intriguingly, insertion between lipids also occurs with egg yolk PG, as well as DMPG monolayers. Altogether, those results allowed us to conclude that the insertion of mtCK into monolayers was neither determined by the anionic phosphoester or phosphodiester polar head configuration nor by the acyl chain composition. The peaks observed in the −0.7 to −1.4 V potential range, corresponding to lipid layer response to potential variations, distinctly decreased for all lipids tested. This has previously been interpreted as lipid layer stabilization after mtCK binding, as previously discussed for bovine heart CL [28].

### 4.5. Average orientation changes of mtCK structural elements upon monolayer binding

Using a simulation model correlating the orientation of α-helical structures and the amide-I/amide-II ratio [46] and hypothesizing that the absorption band between 1650 and 1660 $cm^{-1}$ mainly reflected carbonyl peptide group associated to α-helices, we estimated that, whatever the presence of a TMCL, or saturated or unsaturated PG monolayers, the average angle of carbonyl peptide groups associated to α-helices was tilted by 40° with respect to the interface plane. This value is intermediate between the values estimated for the protein alone accumulating at the air–buffer interface (30°), and for the protein in the presence of a bovine heart CL monolayer (45°) [28]. Consequently, whatever the anionic polar head structure and the chain composition, mtCK membrane binding was followed by protein domain movements. The highest amplitude of the tilt was recorded for unsaturated bovine heart cardiolipin.

Both PG and DMPG are considered as cylindrical shaped lipids in which the orientation of the polar head group may be similar. Cardiolipins, on the other hand, are generally considered as conical shaped phospholipids in which the hydrophobic tail is larger than the polar head group. This discrepancy is even more pronounced for tetralinoleylcardiolipin (the main component of bovine heart CL) due to the double unsaturated acyl chains. We can then imagine that the distance between negatively charged phosphate groups is different in TMCL and bovine heart CL monolayers affecting lipid packing and protein interaction.

It has been proposed that in the known mtCK structures [55,57], the distances between the C-terminal lysine side chains are compatible with the Lys-379/Lys-380 pair being bound to the two charged phosphodiester groups of a single cardiolipin molecule and Lys-369 being bound to another cardiolipin molecule [11]. We can speculate that variation in acyl chains between bovine heart CL and TMCL may induce a different polar head orientation, which may in turn affect docking of the lysine side chains of mtCK onto the charged phospholipid head groups of the membrane lipids, leading to a different orientation of mtCK α-helices with respect to the plane of the lipid monolayer.

### 4.6. Concluding remarks

Membrane morphology after mtCK binding depends on acyl chain unsaturation. A certain degree of fluidity of the lipid monolayer is required for the formation of large, organized lipid–protein complexes. Of interest, a high proportion of unsaturated cardiolipins is reported in tissues where mtCK is also highly expressed, such as cardiac and skeletal muscle [1]. In view of its abundance in the

intermembrane space, it is tempting to attribute to this enzyme a role in associating the highly fluid cardiolipins into more organized regions inside the mitochondrial inner membrane, regions that could be reminiscent of rafts described in the plasma membranes. Several pathophysiological situations are known to alter cardiolipin acyl chains composition. For instance, a low proportion of linoleyl acyl chains has been reported after heart failure [58], oxidized CL species appear during apoptosis [2,59] and a decrease in the percentage of linoleyl chain fraction translates into a loss of mitochondrial integrity [29]. Such changes in CL properties are likely to affect mtCK membrane association within mitochondria with consequences in CL lateral distribution and therefore mitochondrial physiology. This hypothesis is supported by the silencing of mtCK genes expression which severely alters mitochondrial structure [25], suggesting that mtCK is not only an enzyme regulating ATP metabolism but also a protein shaping mitochondrial membrane.

## Acknowledgements

We are very grateful to Dr J. Clavilier for very fruitful suggestions and discussions. We thank Vincent Fitzpatrick for correcting the English. We acknowledge funding from University Lyon 1, CNRS, Région Rhône-Alpes and Agence Nationale de la Recherche.

## References

[1] M. Schlame, D. Rua, M.L. Greenberg, The biosynthesis and functional role of cardiolipin, Prog. Lipid Res. 39 (2000) 257–288.
[2] F. Gonzalvez, E. Gottlieb, Cardiolipin: setting the beat of apoptosis, Apoptosis 12 (2007) 877–885.
[3] F. Gonzalvez, Z.T. Schug, R.H. Houtkooper, E.D. MacKenzie, D.G. Brooks, R.J. Wanders, P.X. Petit, F.M. Vaz, E. Gottlieb, Cardiolipin provides an essential activating platform for caspase-8 on mitochondria, J. Cell Biol. 183 (2008) 681–696.
[4] M. Schlame, D. Otten, Analysis of cardiolipin molecular species by high-performance liquid chromatography of its derivative 1, 3-bisphosphatidyl-2-benzoyl-sn-glycerol dimethyl ester, Anal. Biochem. 195 (1991) 290–295.
[5] M. Schlame, M. Ren, Y. Xu, M.L. Greenberg, I. Haller, Molecular symmetry in mitochondrial cardiolipins, Chem. Phys. Lipids 138 (2005) 38–49.
[6] O. Marcillat, D. Goldschmidt, D. Eichenberger, C. Vial, Only one of the two interconvertible forms of mitochondrial creatine kinase binds to heart mitoplasts, Biochim. Biophys. Acta 890 (1987) 233–241.
[7] H.R. Scholte, P.J. Weijers, E.M. Wit-Peeters, The localization of mitochondrial creatine kinase, and its use for the determination of the sidedness of submitochondrial particles, Biochim. Biophys. Acta 291 (1973) 764–773.
[8] C. Vial, C. Godinot, D. Gautheron, Membranes creatine kinase (E.C.2.7.3.2.) in pig heart mitochondria properties and role in phosphate potential regulation, Biochimie 54 (1972) 843–852.
[9] M. Muller, R. Moser, D. Cheneval, E. Carafoli, Cardiolipin is the membrane receptor for mitochondrial creatine phosphokinase, J. Biol. Chem. 260 (1985) 3839–3843.
[10] M. Schlame, W. Augustin, Association of creatine kinase with rat heart mitochondria: high and low affinity binding sites and the involvement of phospholipids, Biomed. Biochim. Acta 44 (1985) 1083–1088.
[11] U. Schlattner, F. Gehring, N. Vernoux, M. Tokarska-Schlattner, D. Neumann, O. Marcillat, C. Vial, T. Wallimann, C-terminal lysines determine phospholipid interaction of sarcomeric mitochondrial creatine kinase, J. Biol. Chem. 279 (2004) 24334–24342.
[12] O. Maniti, M.F. Lecompte, O. Marcillat, C. Vial and T. Granjon, Mitochondrial creatine kinase interaction with cardiolipin-containing biomimetic membranes is a two-step process involving adsorption and insertion, Eur Biophys J 39 1649–1655.
[13] E. Quemeneur, D. Eichenberger, C. Vial, Immunological determination of the oligomeric form of mitochondrial creatine kinase in situ, FEBS Lett. 262 (1990) 275–278.
[14] C. Vial, O. Marcillat, D. Goldschmidt, B. Font, D. Eichenberger, Interaction of creatine kinase with phosphorylating rabbit heart mitochondria and mitoplasts, Arch. Biochem. Biophys. 251 (1986) 558–566.
[15] A.V. Kuznetsov, V.A. Saks, Affinity modification of creatine kinase and ATP-ADP translocase in heart mitochondria: determination of their molar stoichiometry, Biochem. Biophys. Res. Commun. 134 (1986) 359–366.
[16] P. Riccio, H. Aquila, M. Klingenberg, Purification of the carboxy-atractylate binding protein from mitochondria, FEBS Lett. 56 (1975) 133.
[17] T. Major, B. von Janowsky, T. Ruppert, A. Mogk, W. Voos, Proteomic analysis of mitochondrial protein turnover: identification of novel substrate proteins of the matrix protease pim1, Mol. Cell. Biol. 26 (2006) 762–776.
[18] M. Kottke, V. Adams, I. Riesinger, G. Bremm, W. Bosch, D. Brdiczka, G. Sandri, E. Panfili, Mitochondrial boundary membrane contact sites in brain: points of hexokinase and creatine kinase location, and control of Ca2+ transport, Biochim. Biophys. Acta 935 (1988) 87–102.
[19] M. Kottke, V. Adams, T. Wallimann, V.K. Nalam, D. Brdiczka, Location and regulation of octameric mitochondrial creatine kinase in the contact sites, Biochim. Biophys. Acta 1061 (1991) 215–225.
[20] G. Beutner, A. Ruck, B. Riede, D. Brdiczka, Complexes between porin, hexokinase, mitochondrial creatine kinase and adenylate translocator display properties of the permeability transition pore. Implication for regulation of permeability transition by the kinases, Biochim. Biophys. Acta 1368 (1998) 7–18.
[21] D. Brdiczka, G. Beutner, A. Ruck, M. Dolder, T. Wallimann, The molecular structure of mitochondrial contact sites. Their role in regulation of energy metabolism and permeability transition, Biofactors 8 (1998) 235–242.
[22] D. Brdiczka, P. Kaldis, T. Wallimann, In vitro complex formation between the octamer of mitochondrial creatine kinase and porin, J. Biol. Chem. 269 (1994) 27640–27644.
[23] M. Dolder, B. Walzel, O. Speer, U. Schlattner, T. Wallimann, Inhibition of the mitochondrial permeability transition by creatine kinase substrates. Requirement for microcompartmentation, J. Biol. Chem. 278 (2003) 17760–17766.
[24] O. Speer, N. Back, T. Buerklen, D. Brdiczka, A. Koretsky, T. Wallimann, O. Eriksson, Octameric mitochondrial creatine kinase induces and stabilizes contact sites between the inner and outer membrane, Biochem. J. 385 (2005) 445–450.
[25] H. Lenz, M. Schmidt, V. Welge, T. Kueper, U. Schlattner, T. Wallimann, H.P. Elsasser, K.P. Wittern, H. Wenck, F. Staeb, T. Blatt, Inhibition of cytosolic and mitochondrial creatine kinase by siRNA in HaCaT- and HeLaS3-cells affects cell viability and mitochondrial morphology, Mol. Cell. Biochem. 306 (2007) 153–162.
[26] T. Granjon, M.J. Vacheron, C. Vial, R. Buchet, Mitochondrial creatine kinase binding to phospholipids decreases fluidity of membranes and promotes new lipid-induced beta structures as monitored by red edge excitation shift, laurdan fluorescence, and FTIR, Biochemistry 40 (2001) 6016–6026.
[27] R.F. Epand, M. Tokarska-Schlattner, U. Schlattner, T. Wallimann, R.M. Epand, Cardiolipin clusters and membrane domain formation induced by mitochondrial proteins, J. Mol. Biol. 365 (2007) 968–980.
[28] O. Maniti, M.F. Lecompte, O. Marcillat, B. Desbat, R. Buchet, C. Vial, T. Granjon, Mitochondrial creatine kinase binding to phospholipid monolayers induces cardiolipin segregation, Biophys. J. 96 (2009) 2428–2438.
[29] P.G. Barth, H.R. Scholte, J.A. Berden, J.M. Van der Klei-Van Moorsel, I.E. Luyt-Houwen, E.T. van't Veer-Korthof, J.J. Van der Harten, M.A. Sobotka-Plojhar, An X-linked mitochondrial disease affecting cardiac muscle, skeletal muscle and neutrophil leucocytes, J. Neurol. Sci. 62 (1983) 327–355.
[30] P. Vreken, F. Valianpour, L.G. Nijtmans, L.A. Grivell, B. Plecko, R.J. Wanders, P.G. Barth, Defective remodeling of cardiolipin and phosphatidylglycerol in Barth syndrome, Biochem. Biophys. Res. Commun. 279 (2000) 378–382.
[31] O. Marcillat, C. Perraut, T. Granjon, C. Vial, M.J. Vacheron, Cloning, Escherichia coli expression, and phase-transition chromatography-based purification of recombinant rabbit heart mitochondrial creatine kinase, Prot. Expr. Purif. 17 (1999) 163–168.
[32] B. Font, C. Vial, D. Goldschmidt, D. Eichenberger, D.C. Gautheron, Effects of SH group reagents on creatine kinase interaction with the mitochondrial membrane, Arch. Biochem. Biophys. 220 (1983) 541–548.
[33] D. Hönig, D. Möbius, Direct visualization of monolayers at the air–water interface by Brewster angle microscopy, J. Phys. Chem. 95 (12) (1991) 4590–4592.
[34] S. Henon, J. Meunier, Microscope at the Brewster angle: direct observation of first-order phase transitions in monolayers, Rev. Sci. Instrum. 62 (1991) 936–939.
[35] J.M. Rodriguez Patino, C.C. Sanchez, M.R. Rodriguez Nino, Structural and morphological characteristics of [beta]-casein monolayers at the air–water interface, Food Hydrocolloids 13 (1999) 401.
[36] J.M. Rodriguez Patino, C. Carrera Sanchez, M.R. Rodriguez Nino, Morphological and structural characteristics of monoglyceride monolayers at the air–water interface observed by Brewster angle microscopy, Langmuir 15 (1999) 2484–2492.
[37] P.K. Glasoe, F.A. Long, Use of glass electrodes to measure acidities in deuterium oxide, J. Phys. Chem. (1960) 188–190.
[38] R. Parsons, Equilibrium properties of electrified interphases, in: J.O.M. Bockris, B.E. Conway (Eds.), Modern Aspects of Electrochemistry, Butterworths, London, 1954,, Chapter 3.
[39] M.F. Lecompte, G. Bouix, K.G. Mann, Electrostatic and hydrophobic interactions are involved in factor Va binding to membranes containing acidic phospholipids, J. Biol. Chem. 269 (1994) 1905–1910.
[40] M.F. Lecompte, A.C. Bras, N. Dousset, I. Portas, R. Salvayre, M. Ayrault-Jarrier, Binding steps of apolipoprotein A-I with phospholipid monolayers: adsorption and penetration, Biochemistry 37 (1998) 16165–16171.
[41] M.F. Lecompte, J. Clavilier, C. Rolland, X. Collet, A. Negre-Salvayre, R. Salvayre, Effect of 4-hydroxynonenal on phosphatidylethanolamine containing condensed monolayer and on its interaction with apolipoprotein A-I, FEBS Lett. 579 (2005) 5074–5078.
[42] M.F. Lecompte, Interaction of an amphitropic protein (factor Xa) with membrane models in a complex system, Biochim. Biophys. Acta 1724 (2005) 307–314.
[43] D. Blaudez, J.M. Turlet, J. Dufourcq, D. Bard, T. Buffeteau, B. Desbat, Investigations at the air/water interface using polarization modulation IR spectroscopy, J. Chem. Soc. Faraday Trans. 92 (1996) 525–530.
[44] D. Blaudez, T. Buffeteau, J.C. Cornut, B. Desbat, N. Escafre, M. Pézolet, J.M. Turlet, Polarization modulation FTIR spectroscopy at the air–water interface, Thin Solid Films 242 (1994) 146–150.
[45] S. Castano, B. Desbat, J. Dufourcq, Ideally amphipathic beta-sheeted peptides at interfaces: structure, orientation, affinities for lipids and hemolytic activity of (KL)(m)K peptides, Biochim. Biophys. Acta 1463 (2000) 65–80.

[46] S. Castano, B. Desbat, M. Laguerre, J. Dufourcq, Structure, orientation and affinity for interfaces and lipids of ideally amphipathic lytic LiKj(i = 2j) peptides, Biochim. Biophys. Acta 1416 (1999) 176–194.
[47] D. Ducharme, J.J. Max, C. Salesse, R.M. Leblanc, Ellipsometric study of the physical states of phosphatidylcholines at the air–water interface, J. Phys. Chem. 94 (1990) 1925–1932.
[48] L.A. Bagatolli, T. Parasassi, G.D. Fidelio, E. Gratton, A model for the interaction of 6-lauroyl-2-(N, N-dimethylamino)naphthalene with lipid environments: implications for spectral properties, Photochem. Photobiol. 70 (1999) 557–564.
[49] T. Parasassi, F. Conti, E. Gratton, Time-resolved fluorescence emission spectra of Laurdan in phospholipid vesicles by multifrequency phase and modulation fluorometry, Cell. Mol. Biol. 32 (1986) 103–108.
[50] T. Parasassi, G. De Stasio, A. d'Ubaldo, E. Gratton, Phase fluctuation in phospholipid membranes revealed by Laurdan fluorescence, Biophys. J. 57 (1990) 1179–1186.
[51] L.A. Bagatolli, To see or not to see: lateral organization of biological membranes and fluorescence microscopy, Biochim. Biophys. Acta 1758 (2006) 1541–1556.
[52] A. Nelson, F.A.M. Leermakers, Substrate-induced structural changes in electrode-adsorbed lipid layers. Experimental evidence from the behaviour of phospholipid layers on the mercury–water interface, J. Electroanal. Chem. 278 (1990) 73–83.
[53] N. Vernoux, O. Maniti, O. Marcillat, C. Vial, T. Granjon, Mitochondrial creatine kinase interaction with heterogeneous monolayers: effect on lipid lateral organization, Biochimie 91 (2009) 752–764.
[54] O. Maniti, M. Cheniour, O. Marcillat, C. Vial, T. Granjon, Morphology modifications in negatively charged lipid monolayers upon mitochondrial creatine kinase binding, Mol. Membr. Biol. 26 (2009) 171–185.
[55] K. Fritz-Wolf, T. Schnyder, T. Wallimann, W. Kabsch, Structure of mitochondrial creatine kinase, Nature 381 (1996) 341–345.
[56] S.C. Chang, P.N. Heacock, E. Mileykovskaya, D.R. Voelker, W. Dowhan, Isolation and characterization of the gene (CLS1) encoding cardiolipin synthase in Saccharomyces cerevisiae, J. Biol. Chem. 273 (1998) 14933–14941.
[57] M. Eder, K. Fritz-Wolf, W. Kabsch, T. Wallimann, U. Schlattner, Crystal structure of human ubiquitous mitochondrial creatine kinase, Proteins 39 (2000) 216–225.
[58] G.C. Sparagna, A.J. Chicco, R.C. Murphy, M.R. Bristow, C.A. Johnson, M.L. Rees, M.L. Maxey, S.A. McCune, R.L. Moore, Loss of cardiac tetralinoleoyl cardiolipin in human and experimental heart failure, J. Lipid Res. 48 (2007) 1559–1570.
[59] Z.T. Schug, E. Gottlieb, Cardiolipin acts as a mitochondrial signalling platform to launch apoptosis, Biochim. Biophys. Acta 1788 (2009) 2022–2031.